ELSEVIER

Polymer 41 (2000) 5431–5435

polymer

Microhardness studies of chain-extended PE: III. Correlation with yield stress and elastic modulus

A. Flores[a], F.J. Baltá Calleja[a,*], G.E. Attenburrow[b,1], D.C. Bassett[b]

[a]*Instituto de Estructura de la Materia, C. S. I. C., Serrano 119, 28006 Madrid, Spain*
[b]*J.J. Thomson Laboratory, University of Reading, Whiteknights, Reading RG6 6AF, UK*

Received 26 July 1999; accepted 14 October 1999

Abstract

The correlation between microhardness, H, yield stress, Y, and Young's modulus, E, has been explored on various chain-extended polyethylene (PE) samples and compared to chain-folded PE. Mechanical properties have been derived from tensile and compressive experiments. The tensile yield stress, Y_t, is shown to correlate with hardness following $H \sim 3Y_t$ while $H \sim E_t/10$ (E_t is Young's modulus derived from tensile experiments). On the other hand, the compressive yield stress, Y_c, is shown to correlate to H following the mechanical models of elastoplastic indentation. Hence, H/Y_c increases with decreasing elastic strain tending towards $H \sim 3Y_c$ for a fully plastic deformation. The atmospheric pressure compression-moulded samples show the lowest H/Y_c ratios as a consequence of the largest fraction of compliant phase. Moreover, the H/E_c ratio (E_c being the elastic modulus under compressive force) is shown to diminish with the decrease of Y_c/E_c. Chain extended PE provides the lowest values for the H/E_c ratio from all the PE samples investigated.

Keywords: Microhardness; Yield stress; Elastic modulus

1. Introduction

During the last two decades investigation of the microhardness properties of polymers has evolved from topics of applied significance [1–3] to more basic studies aiming to gain a deeper understanding of the microhardness-morphology correlation in these materials [4–6]. The direct influence of crystal thickness upon microhardness was recognized early [7] and later verified in many chain-folded lamellar examples [8–10]. In part I of this series [11], we dealt with the influence of morphological aspects of chain-extended polyethylene (CEPE) (lamellar thicknesses in the micron range) on microhardness. CEPE, achieved by high pressure annealing or crystallization [12,13], shows enhanced mechanical properties with respect to chain-folded PE produced under atmospheric conditions. The outstanding hardness values found for CEPE are a consequence of the unusually large lamellar thickness and high degrees of crystallinity. Part II was devoted to the study of the creep behaviour of the CEPE samples and their chain-folded counterparts [14], the main conclusion being that lamellar thickness is the dominant variable controlling the time dependence of indentation. It was shown that the micromechanical behaviour of each PE sample can be unambiguously defined in terms of a creep constant k and a microhardness value defined at a given reference time [14].

The Young's modulus and the fracture behaviour of oriented CEPE were the object of an early investigation [15]. The modulus was shown to be sensitive to the textural changes occurring when the drawn polymer is annealed at different temperatures [15].

The present work complements the preceding mechanical investigations on isotropic CEPE and raises the question of the microhardness correlation with macroscopic mechanical properties (yield stress and Young's modulus). Results are discussed in the light of several mechanical models relating the microhardness to yield stress and Young's modulus.

2. Mechanical models

According to Tabor, the indentation pressure, P_m, across the surface of a flat punch is approximately equal to three times the yield stress, Y, in frictionless compression [16]. For a Vickers diamond pyramid, the ratio between P_m and Y

* Corresponding author.
[1] Now at The British School of Leather Technology, University College Northampton NN2 7AL, UK.

0032-3861/00/$ - see front matter
PII: S0032-3861(99)00755-7

Table 1
Yield stress and Young's modulus in tension and compression for the PE samples investigated

Sample		Processing conditions	H (MPa)	Y_t (MPa)	E_t (MPa)	Y_c (MPa)	E_c (MPa)
$M_w = 1.55 \times 10^5$ g/mol	Chain-folded	Compression moulded	47	23.5	353	30.1	537
		$T_a = 127$°C $t_a = 12$ min	77	25.8	458	37.5	700
		$T_a = 127$°C $t_a = 1$ h	74	25.4	552	39.0	840
		$T_a = 127$°C $t_a = 96$ h	86	28.7	766	43.5	1165
H02054P	Chain-extended	Crystallised at 260°C (5 kbar)	110	34.2	1317	54.4	2000
$M_w > 2 \times 10^6$ g/mol	Chain-folded	Compression moulded	31	15.1	219	18.6	333
		$T_a = 127$°C $t_a = 96$ h	45	16.8	348	24.4	530
	Chain-extended	Annealed at 235°C (5.3 kbar)	76	27.7	601	34.8	915
		Annealed at 245°C (5.3 kbar)	107	34.4	931	57.4	1415
		Crystallised at 260°C (5 kbar)	84	20.3	1620	41.0	2470

takes a value of about 3.3 ($H = 0.927\, P_m$) [16]. This relation applies for work-hardened metals, which behave as ideally plastic materials, but fails for other metals, glasses and polymers where the elastic strains are non-negligible [17,18].

Marsh was the first one to suggest that an elastoplastic indentation is similar to the expansion of a spherical cavity under hydrostatic pressure in an infinite elastic–plastic medium [17]. In this simplified model, the indentation pressure is related to the yield stress and elastic modulus, E, through:

$$\frac{P_m}{Y} = C + KB \ln Z \tag{1}$$

where C and K are constants and B and Z are related to the Y/E ratio through Poisson's ratio, ν. Marsh showed that for a high value of the Y/E ratio (highly elastic materials), the change to a radial flow mode of deformation would occur more easily (low P_m/Y values). Using a Vickers indenter, expression (1) was shown to be valid for a wide variety of materials, ranging from metals to glasses and polymers, leading to best-fit values of $C = 0.28$ and $K = 0.60$. The C and K constants allow for the correction for the possible elastic contraction of the impression on unloading.

Following the expansion cavity theory, Johnson proposed a model [19] where the contact surface of the indenter is encased within a hemi-spherical core. The hemi-spherical core of radius a is immediately followed by a plastic zone. The plastic–elastic boundary lies here at a radius c, where $c > a$. The model allows the P_m/Y ratio to be related to a single non-dimensional variable $E \tan \beta/Y$, where β is the contact angle between the sample and the indenter ($\beta = 19.7°$ for a Vickers indenter). For $\nu = 0.5$, Johnson's analysis leads to:

$$\frac{P_m}{Y}\frac{2}{3}\left[2 + \ln\left(\frac{E \tan \beta}{3Y}\right)\right]. \tag{2}$$

An additional term in the argument of the logarithm should be introduced for ν values other than 0.5. Studman et al. [20] and Perrot [21] eliminated certain simplifying assumptions used in Johnson's analysis. These two last approaches lead to a modified form of Eq. (2) which still relates P_m/Y linearly to $\ln(E \tan \beta/Y)$ for $\nu = 0.5$ but which requires new values for the numerical factors.

3. Experimental

3.1. Samples

We used standard linear unfractioned PE (Rigidex 9) with $M_n = 1.17 \times 10^4$ g/mol and $M_w = 1.55 \times 10^5$ g/mol and high molecular weight PE (Hifax 1900) with $M_w > 2 \times 10^6$ g/mol as used in parts I and II. In addition, a higher molecular weight grade of PE, Rigidex H02054P, was also used for high pressure crystallization because it was not prone to giving segregated populations of short molecules under these circumstances. Two morphologies were investigated: the first was ordinary chain folded lamellae i.e. compression moulded material crystallized from the melt as described in the preceding paper [11]. Annealing of the original moulded sheets was by immersing the specimens in a glycerine bath at 127°C for a specific period of time (ranging from 12 min to 96 h) following the procedure described in part I [11]. The second material was CEPE obtained by crystallization or annealing at 5 kbar [11].

3.2. Techniques

Microhardness measurements were performed at room temperature (~21°C) using a Vickers diamond pyramid (included angle $2\alpha = 136°$). Hardness was measured from the diagonal of the residual indentation as described in preceding reviews [5,9]. Loads ranging from 147–981 mN were used to correct for the instant elastic recovery. An indentation time of 0.1 min was used to minimize for the creep effect. The resulting deformation was measured immediately after load release in order to avoid complications associated with viscoelastic recovery.

Dumbbells shaped samples for tensile testing were cut. All specimens had a gauge length of 1.0 cm and widths of 3–4 mm except for two specimens with a gauge length of 2.5 and 0.4 cm, both with a width of 1.5 cm. Specimen thickness varied between 0.7 and 1.3 mm. Load extension curves were obtained using an Instron table 1115 machine

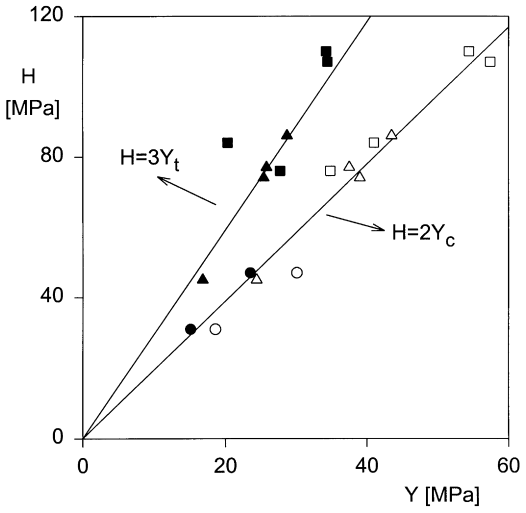

Fig. 1. Variation of hardness with tensile (solid symbols) and compressive yield stress (open symbols). ○, ●: compression moulded samples; △, ▲: annealed samples at atmospheric pressure; □, ■: chain-extended samples.

operated at a crosshead speed of 0.05 cm min^{-1}. The crosshead velocity was chosen to be comparable to the strain rate in the hardness tests [22]. From these experiments, the initial Young's modulus, E_t, and true tensile yield stress, Y_t, were calculated.

Specimens in the form of flat plates ~1 mm thick were subjected to a plane strain compression test described by Williams and Ford [23]. This procedure consists of compressing the specimen between two parallel dies 5 cm long by 2.55 mm wide and lubricated with petroleum jelly to give negligible friction. The specimen plate width varied between 2 and 6 mm (depending on the availability of the material). At least three specimens of each type were tested. The advantage of this test is that the area under compression remains constant. Load compression curves were obtained

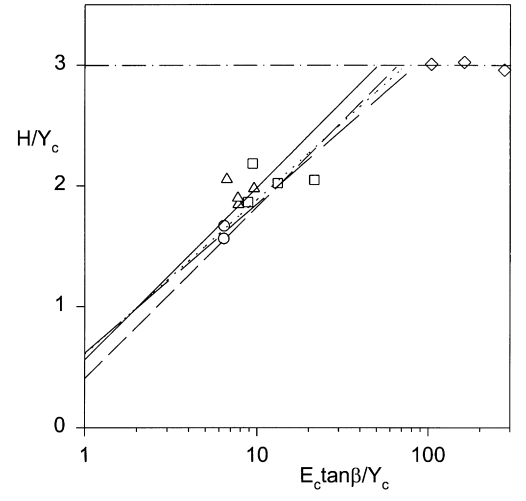

Fig. 2. Plot of H/Y_c vs. $\log(\tan\beta E_c/Y_c)$ for: ○, compression moulded PE; △, annealed PE at atmospheric pressure; □, CEPE; ◇, work-hardened metals [16]. The straight lines follow the theoretical models of elastoplastic indentation from: ·····Marsh [17]; —Johnson [19]; – – – Studman et al. [20]; — — Perrot [21].

using an Instron compression load cell and placing the dies between the Instron compression plates. The crosshead speed was 0.01 cm min^{-1}. Values for Y_c were obtained from these experiments. E_c was estimated from $E_c \approx (Y_c/Y_t)E_t$ assuming that the elastic strains at the yield point in a compressive and tensile test are roughly the same.

Table 1 collects the values of H, Y_c, E_c, Y_t and E_t for the chain-folded and chain-extended PE samples investigated.

4. Results and discussion

4.1. Hardness to yield stress correlation

Fig. 1 shows the plot of H as a function of the tensile yield stress (solid symbols) and the compressive yield stress (open symbols) for the samples investigated. In both cases, the higher H and Y values correspond to chain-extended samples while the lower ones are associated to the starting chain-folded material (see Ref. [11] for a detailed discussion). It is seen that in all cases Y_c is larger than Y_t. This difference has been ascribed to the effect of the hydrostatic component of stress on isotropic polymers including PE [24]. The data in Fig. 1 fit into two straight lines which pass through the origin yielding $H/Y_t \sim 3$ and $H/Y_c \sim 2$. Previous investigations carried out in our laboratory on melt crystallized PE already indicated that $H \sim 3Y_t$ when the strain rate in the tensile tests is comparable to that employed in the hardness tests [22]. A closer inspection of Fig. 1 reveals slight deviations from $H/Y_t \sim 3$, the original moulded samples exhibiting values $H/Y_t \sim 2$ while the chain-extended samples show H/Y_t ~3–4. On the other hand, the H/Y_c ratio considerably deviates from that predicted by the theory of plasticity ($H/Y_c \sim 3$) even for highly crystalline samples such as CEPE, where one would expect the elastic strains to be minimised.

4.2. Comparison with elastoplastic models

The above results evidence the elastoplastic response to indentation of all the PE samples investigated. Hence, it is convenient to discuss the hardness correlation with the yield stress in the light of the various models developed to account for the elastic–plastic strains under a compressive stress. Fig. 2 shows the semi-logarithmic plot of the H/Y_c versus $E_c \tan\beta/Y_c$ data for all the PE samples investigated. The E_c/Y_c ratio is a measure of the reciprocal value of the elastic strain of the material. Hence, the observed tendency of the H/Y_c values to increase towards $H \sim 3Y_c$ (ideal plastic behaviour) can be related to a decrease of elastic strains. The H/Y_c ratio is lowest for the compression moulded (chain-folded) samples, where the fraction of compliant (amorphous) phase is the highest. The various straight lines plotted in Fig. 2 are drawn according to the different models of elastoplastic indentation (using $H = 0.927\,P_m$). In our calculations, we have used the approximation $\nu = 0.5$. The theoretical straight lines in Fig. 2 are represented

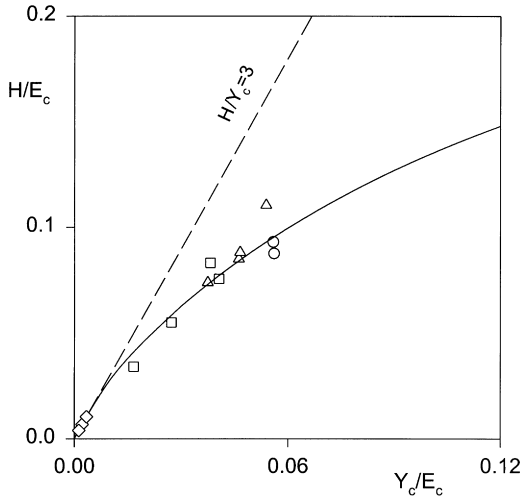

Fig. 3. Plot of H/E_c as a function of Y_c/E_c for all the PE samples investigated. Data for work-hardened metals are included for comparison. Symbols as in Fig. 2. The theoretical curve is drawn according to Johnson [19].

within the region of elastoplastic contact. This approximately comprises H/Y_c values from 0.5 (first yield for a Vickers indenter occurs at $P_m \sim 0.5\,Y$ [19]) up to three (fully plastic deformation). Along the abscissa, for $E_c \tan\beta/Y_c$ values higher than 40–60, the rigid-plastic mode of deformation prevails while for $E_c \tan\beta/Y_c < 1$, the response is largely elastic. Data for some work-hardened metals have been also included in Fig. 2 to illustrate the H–Y_c correlation for fully plastic materials, $H = 3Y_c$ (horizontal dashed-dotted line).

The theoretical straight lines in Fig. 2 agree reasonably well with the experimental data for all the PE samples investigated. The best fit possibly corresponds to Johnson's model although the difference with other approaches is small within the range of H/Y_c values considered.

According to Johnson's model, the P_m/E_c ratio is described through:

$$\frac{P_m}{E_c} = \frac{Y_c}{E_c}\frac{2}{3}\left[2 + \ln\left(\frac{E_c \tan\beta}{3Y_c}\right)\right]. \quad (3)$$

Analogous equations can be derived for the mechanical models of Marsh [17], Studman [20] and Perrot [21]. Fig. 3 represents the theoretical curve described in Eq. (3) relating P_m/E with Y_c/E_c and using a value of $H = 0.927\,P_m$. Data for work-hardened metals are included together with the straight line indicating the fully plastic behaviour (dashed line). For $Y_c/E_c < 0.01$ ($E_c \tan\beta/Y_c > 40$), the material behaves as ideally plastic and Tabor's relation applies ($H/Y_c \sim 3$). The data plotted in Fig. 3 for all the PE samples investigated are shown to be in good agreement with Eq. (3). As the Y_c/E_c ratio diminishes towards the fully plastic deformation, the H/E_c values decrease. Chain-extended PE shows the lowest Y_c/E_c values in agreement with the higher crystallinity values found for this material.

4.3. Hardness to elastic modulus correlation

Fig. 4 illustrates the H vs. E_t values for all the PE samples investigated. Data from other melt crystallized PE samples (taken from Ref. [25]) have been also included. Microhardness shows a general tendency to increase with increasing elastic modulus. In the previous section we found $H \sim 3\,Y_t$. Moreover, Struik developed a model on account of the intermolecular forces between two molecules, which relates the yield stress to the elastic modulus offering the prediction [26]:

$$Y \approx E/30. \quad (4)$$

Struik successfully tested Eq. (4) for various semicrystalline and amorphous polymers subjected to tensile experiments. If we make use of Eq. (4) together with $H = 3\,Y_t$, then we obtain $H \approx E/10$. This correlation has been represented in Fig. 4 by a straight line. The experimental data corresponding to chain-folded PE are in fair agreement with $H = E_t/10$. However, data for CEPE, most especially for CEPE with high molecular weight ($E = 1620$ MPa), show severe deviations from the theoretical predictions. This result seems to imply that lamellar thickness is here no longer the dominant morphological factor. In the case of chain-extended material, lamellar connectedness plays instead a more decisive role in determining the E value. The main reason for ductility in ultrastiff CEPE has to be sought, in fact, in the strength and toughness of the interlamellar material, which directly increases with the number of interlamellar connections [27].

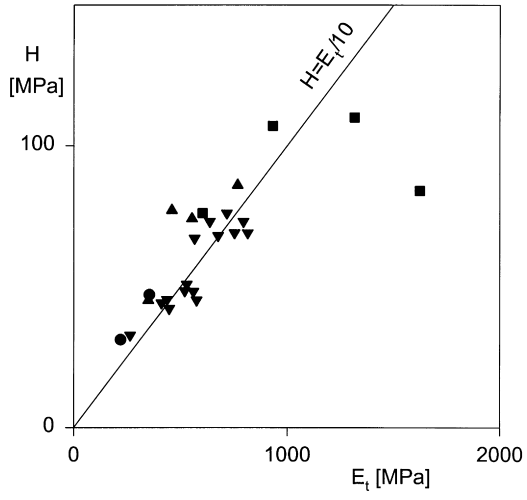

Fig. 4. H variation with E_t for: ●, compression moulded PE; ▲, annealed PE at atmospheric pressure; ■ CEPE; ▼, melt crystallised (chain-folded) PE as taken from Ref. [25].

5. Conclusions

1. For melt crystallized and chain-extended PE with a wide

range of morphologies we find the relationship: $H \sim 3\,Y_t$ provided the strain rates employed in the tensile and indentation tests are comparable.

2. For the yield stress in compression, deviations from Tabor's relation giving values $H \sim 2\,Y_c$ are found. This is presumably due to the elastic strain of the indented material. A detailed analysis of the H/Y_c ratio on the basis of mechanical models of elastoplastic indentation reveals that H/Y_c linearly increases with $\ln(\tan \beta E_c/Y_c)$. Compression moulded (chain-folded) PE samples, which present the lowest crystallinity of all the samples investigated, also show the lowest H/Y_c ratio as a consequence of the comparatively large elastic strains.
3. The H/E_c ratio is shown to decrease with decreasing Y_c/E_c ratio following the theoretical prediction for elastoplastic indentation. CEPE shows the lowest H/E_c values in agreement with an enhanced plastic behaviour in contrast to chain-folded PE.
4. Hardness is related to Young's modulus, as derived from tensile experiments, through $H \sim E_t/10$, in agreement with Struik's model predictions of $Y \sim E/30$.

Acknowledgements

We are indebted to DGICYT (Grant PB94-0049) Spain, for the generous support of this investigation. One of us (AF) thanks the Comunidad Autónoma de Madrid for the award of a postdoctoral grant.

References

[1] Eyerer P, Lang G. Kunststoffe 1972;62:322.
[2] May M, Fröhlich F, Grau P, Grellmann W. Plaste und Kautschuk 1983;30:149.
[3] Darlix B, Monasse B, Montmitonnet P. Polym Testing 1986;6:107.
[4] Deslandes Y, Alva Rosa E, Brisse F, Meneghini TJ. Mater Sci 1991;26:2769.
[5] Baltá Calleja FJ. Trends Polym Sci 1994;2:419.
[6] Baltá Calleja FJ, Fakirov S. Trends Polym Sci 1997;5:246.
[7] Baltá Calleja FJ. Colloid Polym Sci 1976;254:258.
[8] Baltá Calleja FJ, Kilian HG. Colloid Polym Sci 1985;263:697.
[9] Baltá Calleja FJ. Adv Polym Sci 1985;66:117.
[10] Baltá Calleja FJ, Kilian HG. Colloid Polym Sci 1988;266:29.
[11] Flores A, Baltá Calleja FJ, Bassett DC. J Polym Sci, Polym Phys, Part I of this series 1999; in press.
[12] Bassett DC. Polymer 1976;17:460.
[13] Bassett DC. Principles of polymer morphology, Cambridge: Cambridge University Press, 1981.
[14] Baltá Calleja FJ, Flores A, Ania F, Bassett DC. J Mater Sci, Part II of this series. 2000;35:1.
[15] Bassett DC, Carder DR. Philos Mag 1973;28:535.
[16] Tabor D. Hardness of metals, London: Oxford University Press, 1951.
[17] Marsh DM. Proc R Soc London A 1964;279:420.
[18] Hirst W, Howse MGJW. Proc R Soc London A 1969;311:429.
[19] Johnson KL. Contact mechanics, Cambridge: Cambridge University Press, 1985.
[20] Studman CJ, Moore MA, Jones SE. J Phys D: Appl Phys 1977;10:949.
[21] Perrott CM. Wear 1977;45:293.
[22] Baltá Calleja FJ, Giri L, Ward IM, Cansfield DLM. J Mater Sci 1995;30:1139.
[23] Williams JG, Ford HJ. Mech Engng Sci 1964;6:405.
[24] Ward IM. J Polym Sci C 1971;32:195.
[25] Santa Cruz C. PhD Thesis. Universidad Autónoma de Madrid, 1991.
[26] Struik LCE. J Non-Cryst Solids 1991;395:131–3.
[27] Attenburrow GE, Bassett DC. J Mater Sci 1977;12:192.